Molecular Cancer Therapeutics

Efficient Payload Delivery by a Bispecific Antibody–Drug Conjugate Targeting HER2 and CD63

Bart E.C.G. de Goeij[1], Tom Vink[1], Hendrik ten Napel[1], Esther C.W. Breij[1], David Satijn[1], Richard Wubbolts[2], David Miao[3], and Paul W.H.I. Parren[1,4,5]

Abstract

Antibody–drug conjugates (ADC) are designed to be stable in circulation and to release potent cytotoxic drugs intracellularly following antigen-specific binding, uptake, and degradation in tumor cells. Efficient internalization and routing to lysosomes where proteolysis can take place is therefore essential. For many cell surface proteins and carbohydrate structures on tumor cells, however, the magnitude of these processes is insufficient to allow for an effective ADC approach. We hypothesized that we could overcome this limitation by enhancing lysosomal ADC delivery via a bispecific antibody (bsAb) approach, in which one binding domain would provide tumor specificity, whereas the other binding domain would facilitate targeting to the lysosomal compartment. We therefore designed a bsAb in which one binding arm specifically targeted CD63, a protein that is described to shuttle between the plasma membrane and intracellular compartments, and combined it in a bsAb with a HER2 binding arm, which was selected as model antigen for tumor-specific binding. The resulting bsHER2xCD63$_{his}$ demonstrated strong binding, internalization and lysosomal accumulation in HER2-positive tumor cells, and minimal internalization into HER2-negative cells. By conjugating bsHER2xCD63$_{his}$ to the microtubule-disrupting agent duostatin-3, we were able to demonstrate potent cytotoxicity of bsHER2xCD63$_{his}$-ADC against HER2-positive tumors, which was not observed with monovalent HER2- and CD63-specific ADCs. Our data demonstrate, for the first time, that intracellular trafficking of ADCs can be improved using a bsAb approach that targets the lysosomal membrane protein CD63 and provide a rationale for the development of novel bsADCs that combine tumor-specific targeting with targeting of rapidly internalizing antigens. *Mol Cancer Ther; 15(11); 2688–97. ©2016 AACR.*

Introduction

Antibody–drug conjugates (ADC) are emerging as powerful anticancer treatments. Over 50 different ADCs are currently in clinical evaluation, while brentuximab vedotin (Adcetris) and trastuzumab emtansine (Kadcyla) have already been approved for the treatment of Hodgkin lymphoma and metastatic breast cancer, respectively (1). These ADCs, as well as virtually all other ADCs in clinical development, are designed to be stable in circulation and to release their cytotoxic payload after internalization and lysosomal processing of the antigen/ADC complex (2). The requirement for antigen- and antibody-mediated internalization limits the number of suitable ADC targets. In many cases, intracellular processing of ADCs is inefficient. Following internalization, receptors such as transferrin (3), HER2 (4, 5), cell adhesion molecule L1 (6), and integrins (7) are continuously recycled back from the endosomal compartment to the plasma membrane. High antigen expression and highly toxic payloads are required to ensure activity of ADCs. Therefore, approaches that increase internalization, lysosomal targeting, and intratumoral processing of ADCs are highly desired.

We previously demonstrated that ADCs that are more efficiently internalized and transported to the lysosomes induce more effective cytotoxicity (8). Therefore, we set out to improve ADC-mediated drug release by improving their intracellular delivery. We generated an ADC based on a bispecific antibody (bsAb; ref. 9), in which one binding arm was responsible for tumor cell binding and the other binding arm was designed to facilitate internalization and lysosomal delivery of the toxic payload. Ideally, such a bispecific ADC (bsADC) would allow utilization of tumor antigens that do not or poorly internalize for an ADC approach, thereby greatly enhancing the pool of potential ADC targets. An antibody specific for the lysosome-associated membrane glycoprotein 3 (LAMP3 or CD63) was selected to provide a Fab arm that facilitates internalization and lysosomal transport. CD63 is a member of the tetraspanin superfamily and is ubiquitously expressed. The major pool of CD63 resides in intracellular compartments such as endosomes and lysosomes, but some expression can be found on the cell surface. Although the biology of CD63 is not completely understood, CD63 has been described to regulate transport of other proteins typically through endocytosis (10). For example, complex formation between CD63 and the gastric H,K-ATPase β-subunit results in the redistribution of H,

[1]Genmab, Utrecht, the Netherlands. [2]Department of Biochemistry and Cell Biology, Faculty of Veterinary Medicine, Utrecht University, Utrecht, the Netherlands. [3]Concortis Biosystems Corp., San Diego, California. [4]Department of Cancer and Inflammation Research, Institute of Molecular Medicine, University of Southern Denmark, Odense, Denmark. [5]Department of Immunohematology and Blood Transfusion, Leiden University Medical Center, Leiden, the Netherlands.

Note: Supplementary data for this article are available at Molecular Cancer Therapeutics Online (http://mct.aacrjournals.org/).

Corresponding Author: Bart E.C.G. de Goeij, Genmab B.V., Yalelaan 60, 3584CM Utrecht, the Netherlands. Phone: 31-302123181; Fax: 31-302123110; E-mail: BGO@genmab.com

doi: 10.1158/1535-7163.MCT-16-0364

K-ATPase from the cell surface to CD63-positive intracellular compartments (11). Furthermore, CD63 has been described to regulate surface expression of membrane-type 1 matrix metalloproteinase by targeting the enzyme for lysosomal degradation (12), and silencing of CD63 in endothelial cells prevents internalization of vascular endothelial growth factor receptor 2 (VEGFR2) in response to its ligand VEGF (13). Also across different tumor types, CD63 has been demonstrated to continuously shuttle between the plasma membrane and lysosomes, which was dependent on the presence of AP2 and clathrin (14). Thus, CD63 seems an attractive antigen to facilitate internalization and lysosomal delivery.

To study our hypothesis that a CD63-specific Ab-arm could promote internalization and lysosomal targeting of a bsAb also including a tumor-specific, poorly internalizing binding arm, we generated a bsAb recognizing CD63 and the human epidermal growth factor receptor 2 (HER2). HER2 is a clinically well-validated ADC target through the clinical experience and approval of trastuzumab emtansine (15). However, for internalization to be most effective HER2 requires cross-linking of HER2 molecules. Especially on tumor cells that highly overexpress HER2, Ab-induced cross-linking has been described to improve internalization of HER2 (5, 16–18). The notion that monomeric HER2 does not internalize well suggested to us that a bsAb with monovalent HER2 binding characteristics may represent a suitable model system for testing whether internalization of cell surface molecules can be increased through binding to CD63.

We found that a bsAb targeting HER2 and CD63 was efficiently transported to lysosomes of HER2-positive tumor cells. This effect was not observed with monovalent control antibodies only targeting HER2 or CD63. By conjugating bsHER2xCD63 with the microtubule disrupting agent duostatin-3, we were able to demonstrate that a bsHER2xCD63-ADC induced potent *in vitro* and *in vivo* cytotoxicity of HER2-positive tumor cells. Monovalent ADCs targeting HER2 or CD63 alone had no effect on tumor growth, which demonstrates that CD63 targeting can be used to improve payload delivery of poorly internalizing ADCs.

Materials and Methods

Cell lines

Human SK-OV-3 (ovarian cancer), HCC1954 (breast ductal carcinoma), and Colo 205 (colorectal adenocarcinoma) cells were obtained from ATCC. SK-OV-3 cells were cultured in Minimal Essential Medium Eagles (ATCC) containing 10% heat-inactivated calf serum (Hyclone). HCC1954 and Colo 205 cells were cultured in RPMI 1640 (Lonza) containing 10% heat-inactivated calf serum. To guarantee cell line authenticity, cell lines were aliquoted and banked, and cultures were grown and used for a limited number of passages before starting a new culture from stock. Cell lines were routinely tested for *mycoplasma* contamination. HER2 cell surface expression was quantified by QIFIKIT analysis (DAKO) according to the manufacturer's guidelines, using a mouse anti-human HER2 antibody (R&D) as described previously (8).

Antibody generation, site-directed mutagenesis, and conjugation

Cloning and production of HER2 antibody IgG1-153 has been described elsewhere (16). The variable domain heavy and light chain regions of integrin β1 antibody huK20 were obtained from WO1996/008564. The variable domain heavy and light chain regions of CD63 antibody 2192 were obtained from hybridoma 2.19 (19), by 5′-RACE of the variable regions from hybridoma derived RNA and sequencing. Variable regions were cloned in the mammalian expression vector pcDNA3.3 (Invitrogen) containing the relevant constant domains (codon optimized; Invitrogen) with the relevant heavy chain constant domain mutations (K409R or F405L). CD63 antibody mutations were introduced either by site-directed mutagenesis or by direct gene synthesis. Antibodies were produced by cotransfection of heavy chain and light chain vectors and transient expression in HEK-293 freestyle cells (Invitrogen) as described by Vink and colleagues (20). Bispecific antibodies (Duobody) were made by controlled Fab-arm exchange as described by Labrijn and colleagues (21). The IgG1-b12 antibody was included as an isotype control (22).

Duostatin-3–conjugated antibodies were generated by covalent conjugation of valine–citrulline–duostatin-3 (Duo3) on antibody lysine groups of IgG1-HER2-F405L and IgG1-b12-F405L as described in WO/2013/173391 and reference 8. After conjugation, IgG1-HER2-F405L-Duo3 and IgG1-b12-F405L-Duo3 were Fab-arm exchanged with IgG1-HER2-K409R, IgG1-CD63-K409R, and IgG1-b12-K409R to generate bsHER2xCD63-Duo3, bsHER2xb12-Duo3, bsCD63xb12-Duo3, IgG1-b12-Duo3, and IgG1-HER2-Duo3 controls, all having an equal DAR of one duostatin-3 molecule per antibody, as determined by hydrophobic interaction chromatography (HIC).

CD63 binding ELISA

The binding of Histidine-mutated IgG1-2192 to CD63 was tested by ELISA. In short, ELISA plates (Greiner) were coated overnight at 4°C with 0.8 μg/mL goat anti-human IgG (The Jackson Laboratory). The plates were blocked with 2% chicken serum and incubated with 1 μg/mL histidine-mutated IgG1-2192. Serially diluted (1–0.0005 μg/mL) recombinant human CD63 (Creative Biomart) was added followed by 1 μg/mL mouse anti-poly-histidine-biotin (R&D Systems). The reaction was visualized using ABTS and stopped with oxalic acid. Fluorescence at 405 nm was measured and depicted using GraphPad Prism 5 software.

CD63 affinity measurements

Kinetics of human His-tagged CD63 (1 μg/mL, 77 nmol/L; Creative BioMart) were assessed using label-free Bio-Layer Interferometry on an Octet RED384 (ForteBio). Anti-CD63 wild-type or mutants containing histidine substitutions were immobilized on Anti-Human IgG Fc Capture Biosensors (ForteBio) at 1 μg/mL. Association and dissociation kinetics were determined in citric acid/Na_2HPO_4 buffer pH7.4 supplemented with 0.1 % BSA Fraction V (Roche) and 0.02% Tween-20 (Sigma-Aldrich), using a shaker speed of 1,000 rpm at 30°C. The dissociation constant K_D (M) was determined with ForteBio Data Analysis v7.0, using the 1:1 model in combination with a local full fit. The six clones with lowest K_D values were measured twice, other clones were measured once.

mAb–FITC accumulation assay with whole blood

Whole blood samples from healthy donors were collected in Heparin tubes. Whole blood was diluted 1:2 in RPMI-1640 supplemented with 10% heat-inactivated cosmic calf serum. CD63 antibodies were conjugated with FITC (Thermo Scientific) according to the manufacturer's instruction and added at a final

concentration of 10 μg/mL, to whole blood cells. Following 1-hour incubation at 4°C or 3 and 16 hours of incubation at 37°C, erythrocytes were lysed by incubating 15 minutes at 4°C with erythrocyte lysis buffer (155 mmol/L NH_4Cl, 10 mmol/L $KHCO_3$, and 0.1 mmol/L EDTA at pH 7.4). Fluorescence intensities of FITC were measured on a flow cytometer (BD). Granulocytes were gated using mouse anti-human CD66b-PerCP-Cy5.5 (BD), and thrombocytes were gated using mouse anti-human CD62-APC (BD).

Confocal microscopy

SK-OV-3 cells were grown on glass coverslips (Thermo Fisher Scientific) at 37°C for 16 hours. One hour prior to antibody treatment, cells were pre-incubated with 50 μg/mL leupeptin (Sigma) to block lysosomal activity. Antibody (1 μg/mL) was added and cells were incubated for 1, 3, or 16 hours at 37°C. Cells were fixed, permeabilized, and incubated 45 minutes with goat anti-human IgG1-FITC (Jackson) to stain for human IgG and mouse anti-human CD107a-APC (BD) to stain for lysosomes. Coverslips were mounted (Calbiochem) on microscope slides and imaged with a Leica SPE-II confocal microscope (Leica Microsystems) equipped with LAS-AF software. 12-bit grayscale TIFF images were analyzed for colocalization using MetaMorph software (Molecular Devices). Colocalization was depicted as arbitrary units (AU) representing the total pixel intensity of antibody overlapping with the lysosomal marker LAMP1. This value was divided by the total pixel intensity of LAMP1, to correct for differences in cell densities between different pictures.

HER2 downmodulation assay

HCC1954, SK-OV-3, and Colo 205 cells were seeded (1 million cells/flask) in T25 flasks (Greiner) and incubated overnight at 37°C to obtain a confluent monolayer. Antibodies were added (10 μg/mL) and cells were cultured for another 3 days at 37°C, washed, and lysed. Total protein levels were quantified using bicinchoninic acid (BCA) protein assay reagent (Pierce), according to the manufacturer's instructions. Next, ELISA plates (Greiner) were coated with 1 μg/mL rabbit anti-human HER2 (Cell Signalling Technology), blocked with 2% chicken serum (Hyclone), and incubated with 50 μL of cell lysate. Goat anti-human HER2-biotin (R&D Systems; 50 ng/mL) was added to detect HER2, followed by streptavidin-poly-HRP (Sanquin; 100 ng/mL). The reaction was visualized using ABTS and stopped with oxalic acid. Fluorescence at 405 nm was measured, and the amount of HER2 was expressed as a percentage relative to untreated cells.

Cytotoxicity assay

Cells were seeded in 96-well tissue culture plates (5,000 cells/well) and incubated for 6 hours at 37°C. Serially diluted ADCs (10–0.0005 μg/mL) were added, and the cells were incubated for 3 days at 37°C. Cell viability was assessed using CellTiter-GLO (Promega), according to the manufacturer's guidelines. The percentage of viable cells was depicted relative to untreated cells.

Tumor xenograft model

Six- to 11-week-old female SCID mice (C.B-17/IcrPrkdc-scid/CRL) were purchased from Charles River. Subcutaneous tumors were induced by inoculation of 5×10^6 SK-OV-3 cells in the right flank of the mice. Tumor volumes were calculated from digital caliper measurements as $0.52 \times \text{length} \times \text{width}^2$ (mm^3). When tumors reached 200 to 400 mm^3, mice were grouped into groups of 7 mice with equal tumor size distribution and mAbs were injected intraperitoneally (8 mg/kg). During the study, blood samples were collected into heparin-containing tubes to confirm the presence of human IgG in plasma. IgG levels were quantified using a nephelometer (Siemens Healthcare). Mice that did not show human IgG in plasma were excluded from the analysis.

Statistical analysis

Data analysis was done using GraphPad Prism 5 software. Group data were reported as mean ± SD. Statistical analysis of xenograft studies was done with one-way ANOVA at the last day when all groups were complete. Mantel–Cox analysis of Kaplan–Meier curves was performed to analyze statistical differences in progression-free survival time.

Results

Generation of a low-affinity CD63 antibody

To improve intracellular trafficking of ADCs, we set out to generate a bsADC that specifically binds to tumor cells with one Fab-arm, while its second Fab-arm is being used to facilitate internalization and lysosomal delivery of the cytotoxic payload. The resulting bsADC should only induce cytotoxicity in tumor cells expressing both antigens. A bsAb targeting HER2 and CD63 was selected as a model for such an ADC. CD63 is ubiquitously expressed and expression is found predominantly in the endosomal and lysosomal compartment, although some expression was also described on the plasma membrane (10, 19). To ensure tumor specificity of the bsAb, the CD63 arm of the bsHER2xCD63 should not bind and internalize in absence of the tumor-specific arm. We hypothesized that a CD63 antibody with low-affinity target binding would fulfill these criteria. Therefore, we first set out to generate a panel of mutated CD63 antibodies with variable CD63 affinity. It has been demonstrated that single amino acid histidine substitutions can be used to alter antibody affinity (23, 24). Hence site-directed mutagenesis was applied to introduce histidine substitutions in the variable heavy and light chain domains of CD63-specific monoclonal antibody 2192. The resulting clones were screened for binding to soluble CD63 with ELISA (Fig. 1A) and label-free Octet (Fig. 1B). Antibodies that showed diminished but detectable binding to CD63 were further analyzed with confocal microscopy to visualize internalization and lysosomal targeting. SK-OV-3 cells were grown on glass coverslips and incubated with histidine-mutated CD63 antibody ($CD63_{his}$). As a control we also tested monovalent bsCD63xb12 that recognizes CD63 with one Fab-arm, while the second Fab-arm recognizes an irrelevant antigen in this context (HIV-1 gp120). After 1- and 16-hour incubation, cells were fixed and permeabilized and human IgG1 was stained with an anti-human IgG-FITC antibody while lysosomes were stained with an anti-LAMP1-APC antibody. Figure 1C–F demonstrates the lysosomal accumulation of the wild-type CD63 antibody and the asparagine into histidine (N74H)-mutated CD63 antibody (IgG1-$CD63_{his}$) that was selected for the development of a low-affinity CD63 arm. After 1-hour incubation, no IgG1-CD63 was detected at the plasma membrane or intracellularly (Fig. 1C). However, after 16 hours of antibody exposure, IgG1-CD63 and the low-affinity IgG1-$CD63_{his}$ were abundantly present in the lysosomes of SK-OV-3 cells, as indicated by the colocalization with LAMP1 (Fig. 1D and F). This

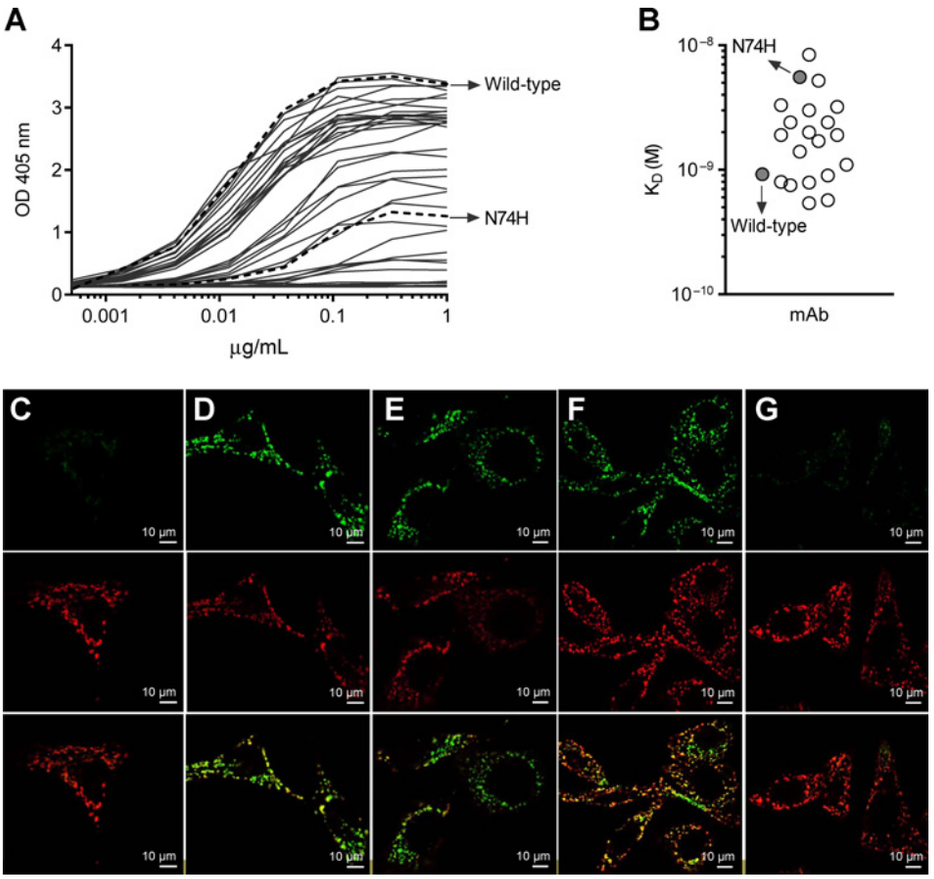

Figure 1.
Binding and intracellular accumulation of CD63 antibody variants. **A,** ELISA plates coated with goat anti-human IgG1 were incubated with a fixed concentration of Histidine-mutated antibody variants of CD63 mAb 2192. Serially diluted recombinant human CD63 was added to determine antibody binding and depicted as OD405 values in correlation to CD63 concentration. The dose response of the selected N74H mutant is indicated. **B,** anti-CD63 antibodies containing histidine substitutions were immobilized on anti-human IgG Fc Capture Biosensors, and the affinity for human His-tagged CD63 was determined using Bio-Layer Interferometry. The dissociation constant K_D (mol/L) was calculated and plotted for each mutant. For a number of antibody variants, the K_D could not be measured accurately because insignificant CD63 binding was detected. As a result, the K_D values of these antibodies are not depicted. **C–G,** SK-OV-3 cells were incubated 1 hour (**C**) or 16 hours (**D–G**) with IgG1-CD63 (**C** and **D**), bsCD63xb12 (**E**), IgG1-$CD63_{his}$(**F**), or bs$CD63_{his}$xb12 (**G**). Lysosomes were stained with mouse anti-human LAMP1-APC (red), and CD63 antibodies were stained with goat anti-human IgG1-FITC (green). Colocalization of anti-human IgG1-FITC with anti-human LAMP1-APC is depicted in orange.

highlights the transient expression of CD63 at the plasma membrane and its constitutive endocytosis and trafficking to the lysosomes. Monovalent bsCD63xb12 also showed substantial transport to lysosomes after 16-hour incubation (Fig. 1E). In contrast, hardly any lysosomal transport was observed for the low-affinity monovalent bs$CD63_{his}$xb12, as shown in Fig. 1G. This indicates the successful generation of a CD63 Fab-arm that should not induce internalization in tissues only expressing CD63.

Binding and internalization of CD63 antibodies in healthy tissue was assessed by measuring intracellular accumulation of FITC-conjugated CD63 antibodies in granulocytes and thrombocytes (10, 19). Whole blood from healthy donors was incubated with FITC-conjugated antibodies for 1 hour at 4°C or for 3 and 16 hours at 37°C. Erythrocytes were lysed, and remaining lymphocytes and thrombocytes were analyzed on a flow cytometer to measure intracellular accumulation of FITC-conjugated antibodies. Figure 2 shows no detectable binding of CD63 antibodies to granulocytes or thrombocytes after 1 hour. However, FITC fluorescence of IgG1-CD63 on granulocytes was clearly increased after 16 hours of incubation, indicating accumulation of IgG1-CD63 into granulocytes. In contrast, FITC fluorescence of bs$CD63_{his}$xb12 was hardly increased after 16 hours. Thus, by using a low-affinity CD63-specific Fab arm, we were able to minimize binding and intracellular accumulation of a monovalent CD63 antibody into healthy cells.

A CD63-specific Fab arm facilitates lysosomal targeting of poorly internalizing antibodies

Next, we investigated whether the $CD63_{his}$-specific Fab arm could be used to facilitate internalization and lysosomal targeting of a HER2-specific Fab arm. HER2 antibody 153 (IgG1-HER2), which is known to internalize as bivalent IgG (16), was used to generate a bispecific IgG1 (bsHER2x$CD63_{his}$) that can bind to both, HER2 and CD63. To validate the use of a monovalent HER2-specific IgG (bsHER2xb12) as a model for an IgG with poor internalization characteristics, we first investigated Ab-induced downmodulation of the monovalent bsHER2xb12. For this, the total amount of HER2 protein in tumor cell lines with different expression levels of HER2, HCC1954 (500,000 HER2/cell), SK-OV-3 (200,000 HER2/cell) and Colo205 (50,000 HER2/cell) was quantified after 3 days of incubation with HER2 antibody and compared with untreated cells. IgG1-HER2 induced ~40% downmodulation of total HER2 in HCC1954 cells that express high levels of HER2 (Fig. 3A), which was in line with previously published results (16). Despite the fact that the monovalent bsHER2xb12 showed dose-dependent binding to HER2-positive cells (Supplementary Fig. S1), no downmodulation of HER2 was observed in the HCC1954 cells (Fig. 3A). This highlights that antibody-dependent receptor cross-linking was critical for increasing the degradation of HER2. The bsHER2x$CD63_{his}$ was able to restore the downmodulation of HER2 on HCC1954 cells. Moreover, on

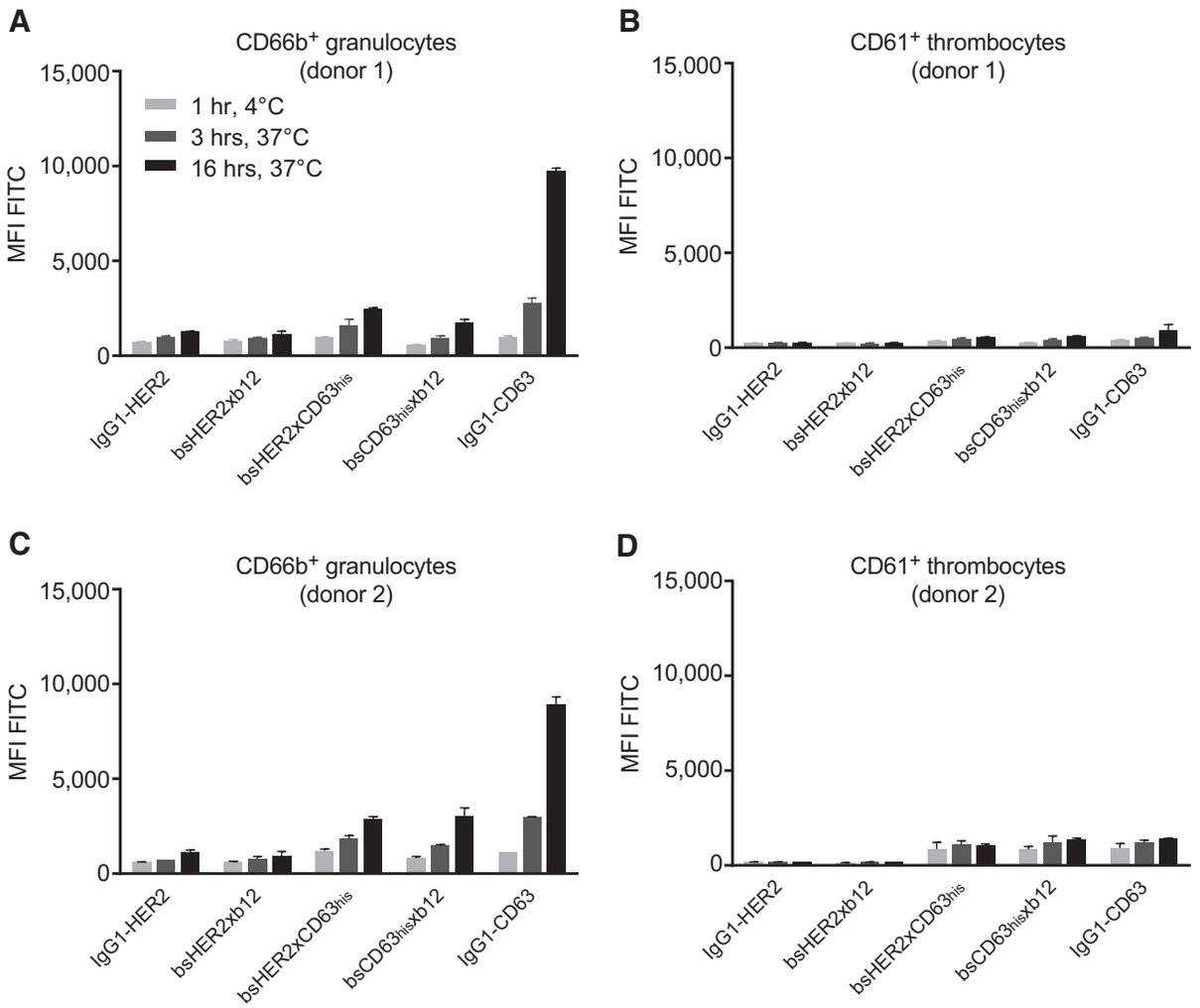

Figure 2.

Binding and intracellular accumulation of IgG1-CD63$_{his}$ in whole blood cells. Whole blood samples from two healthy donors were incubated 1 hour at 4°C, 3 hours at 37°C, or 16 hours at 37°C with 10 μg/mL of FITC-conjugated CD63 antibody. After incubation, erythrocytes were lysed and fluorescence intensities of FITC were measured for the granulocyte (**A** and **C**) and thrombocyte (**B** and **D**) populations using a flow cytometer. Data, mean ± standard deviation of 2 measurements, obtained in two separate donors.

cell lines with lower HER2 expression, such as SK-OV-3 (Fig. 3B) and Colo205 (Fig. 3C), bsHER2xCD63$_{his}$ also induced downmodulation of HER2, whereas IgG1-HER2 did not affect HER2 protein levels.

We next investigated lysosomal transport of bsHER2xCD63$_{his}$ using confocal microscopy. SK-OV-3 cells were incubated with bsAb and left for 1, 3, and 16 hours at 37°C. Following fixation and permeabilization, human IgG1 was stained with an anti-human IgG-FITC antibody and lysosomes were stained with an anti-LAMP1-APC antibody. Figure 4A and B demonstrates that after 1 and 3 hours of incubation, bsHER2xCD63$_{his}$ predominantly localized to the plasma membrane. Whereas after 16 hours (Fig. 4C), plasma membrane staining of bsHER2xCD63$_{his}$ was reduced while colocalization with the lysosomal marker LAMP1 was increased. The lysosomal colocalization of bsHER2xCD63$_{his}$ was more abundant as compared to control Abs only targeting HER2 or CD63 (Fig. 4D and E). These data indicate that binding of bsHER2xCD63$_{his}$ predominantly occurs through interaction with HER2, while interaction with CD63 induces subsequent transport to lysosomes.

To demonstrate that the use of a CD63$_{his}$-specific Fab arm, to facilitate lysosomal transport, is not restricted to HER2 antibodies, we tested lysosomal transport of a bsAb that targets integrin β1 and CD63. Integrin's are known to undergo constant endocytosis; however, they are predominantly recycled back to the plasma membrane without being targeted for lysosomal degradation (25, 26). Supplementary Figure S2 demonstrates that after 1 and 3 hours of incubation, bsβ1xCD63$_{his}$ predominantly localized to the plasma membrane, whereas after 16 hours, all detectable bsβ1xCD63$_{his}$ colocalized with the lysosomal marker LAMP1 (Supplementary Fig. S2C). In contrast, IgG1-β1 was predominantly localized on the plasma membrane after 16

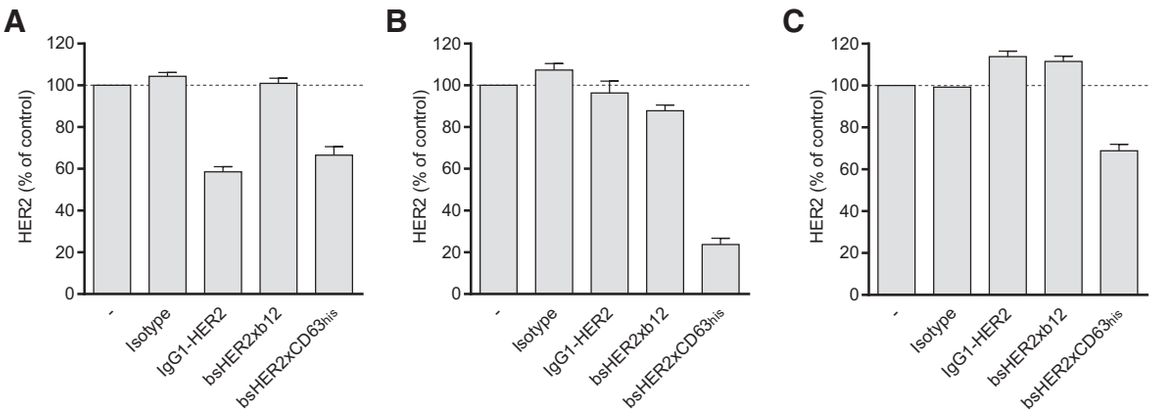

Figure 3.
Antibody-dependent downmodulation of HER2 in tumor cell lines. Relative percentage of HER2 expressed in HCC1954 (**A**), SK-OV-3 (**B**), and Colo205 (**C**) cell lysates after 3 days of incubation with 10 μg/mL antibody. The amount of HER2 was quantified using a HER2-specific capture ELISA and plotted as a percentage relative to untreated cells (−). Data, mean ± standard deviation of 2 experiments.

hours of incubation with antibody (Supplementary Fig. S2D). These results substantiate that the $CD63_{his}$-specific Fab arm can be used to facilitate lysosomal targeting of different tumor antigens.

BsHER2xCD63$_{his}$-duostatin-3 effectively kills HER2-positive tumor cell lines

To investigate whether the strong lysosomal targeting observed with bsHER2xCD63$_{his}$ results in increased cytotoxicity of a

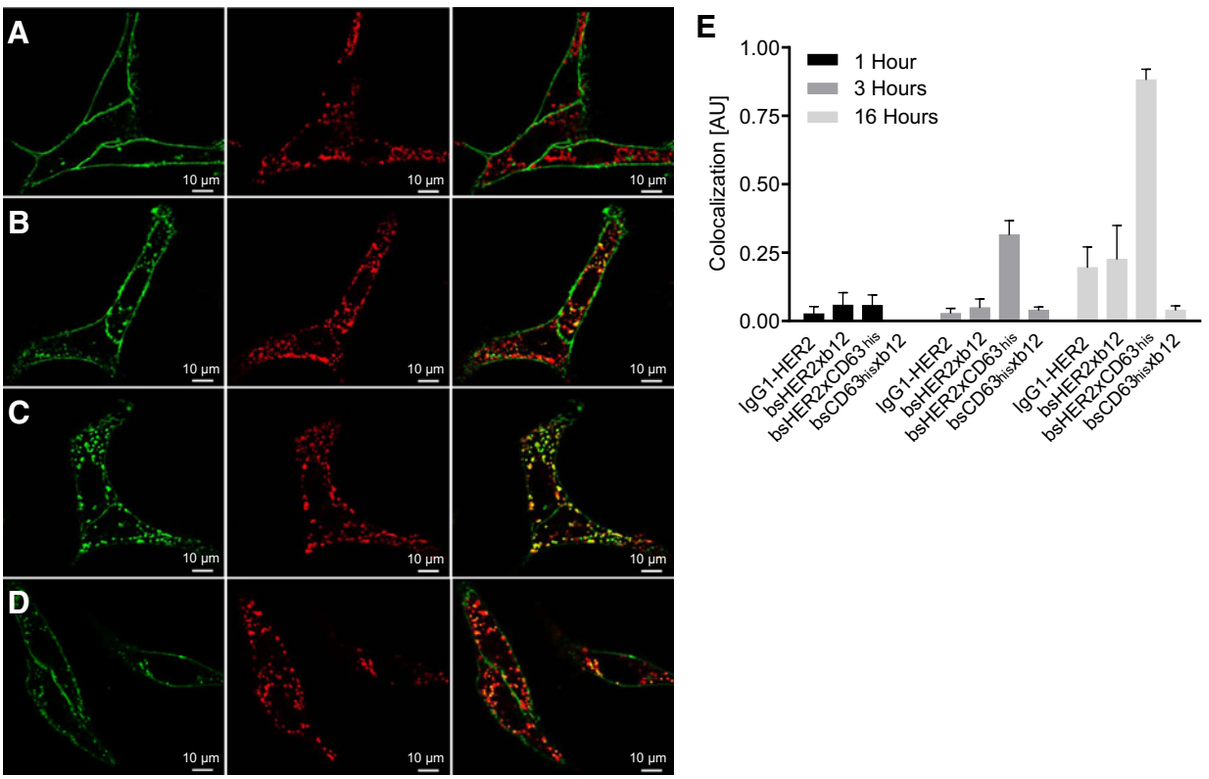

Figure 4.
BsHER2xCD63$_{his}$ colocalizes with lysosomes in SK-OV-3 cells. SK-OV-3 cells were incubated 1 hour (**A**), 3 hours (**B**), or 16 hours (**C** and **D**) with bsHER2xCD63$_{his}$(**A–C**) and bsHER2xb12 (**D**). Lysosomes were stained with mouse anti-human LAMP1-APC (red), and CD63 antibodies were stained with goat anti-human IgG1-FITC (green). Colocalization of anti-human IgG1-FITC with anti-human LAMP1-APC is depicted in orange. **E,** arbitrary units (AU) represent the total pixel intensity of antibody overlapping with the lysosomal marker LAMP1, divided by the total pixel intensity of LAMP1. Data, mean ± standard deviation of 3 images.

bsHER2xCD63$_{his}$-ADC, we conjugated bsHER2xCD63$_{his}$ with the antimitotic agent duostatin-3 (8), using a valine–citrulline linker that is cleaved by lysosomal proteases (27). The resulting duostatin-3–conjugated antibodies were incubated with tumor cell lines, after which cell viability was assessed using CellTiter-GLO. The decrease in viable tumor cells was expressed as a percentage compared to untreated cells. The high HER2-expressing HCC1954 cell line was efficiently killed by bsHER2xHER2-ADC and bsHER2xCD63$_{his}$-ADC (Fig. 5A). The monovalent bsHER2xb12-ADC also induced cytotoxicity of HCC1954 cells, but the IC_{50} value was considerably higher. A marked difference between the ADCs was found on SK-OV-3 cells (Fig. 5B). BsHER2xHER2-ADC and bsHER2xb12-ADC induced modest cytotoxicity of SK-OV-3 cells, while cytotoxicity induced by bsHER2xCD63$_{his}$-ADC was considerably higher. Viability of the low HER2-expressing cell line Colo 205 was not affected by any of the ADCs (Fig. 5C). The cytotoxicity assay with bsHER2xCD63$_{his}$-ADC was also performed in the presence of an excess of unconjugated IgG1-CD63 and unconjugated IgG1-HER2, to block CD63 and HER2 binding at the cell surface, respectively (Fig. 5D). Both conditions increased the IC_{50} value of bsHER2xCD63$_{his}$-ADC induced cytotoxicity, indicating that binding to both HER2 and CD63 at the plasma membrane is required to induce maximal cytotoxicity.

The *in vivo* antitumor activity of a monomeric HER2-ADC is rescued by dual targeting of HER2 and CD63

The strong cytotoxicity of bsHER2xCD63$_{his}$-ADC in SK-OV-3 cells *in vitro* led us to investigate the antitumor effect of bsHER2xCD63$_{his}$-ADC on SK-OV-3 tumor xenografts. SCID mice were inoculated subcutaneously with 5 million SK-OV-3 cells. When tumors reached an average size of 200 mm^3, mice were treated with a single dose of 8 mg/kg ADC. Figure 6 demonstrates that bsHER2xCD63$_{his}$-ADC induced significant inhibition of

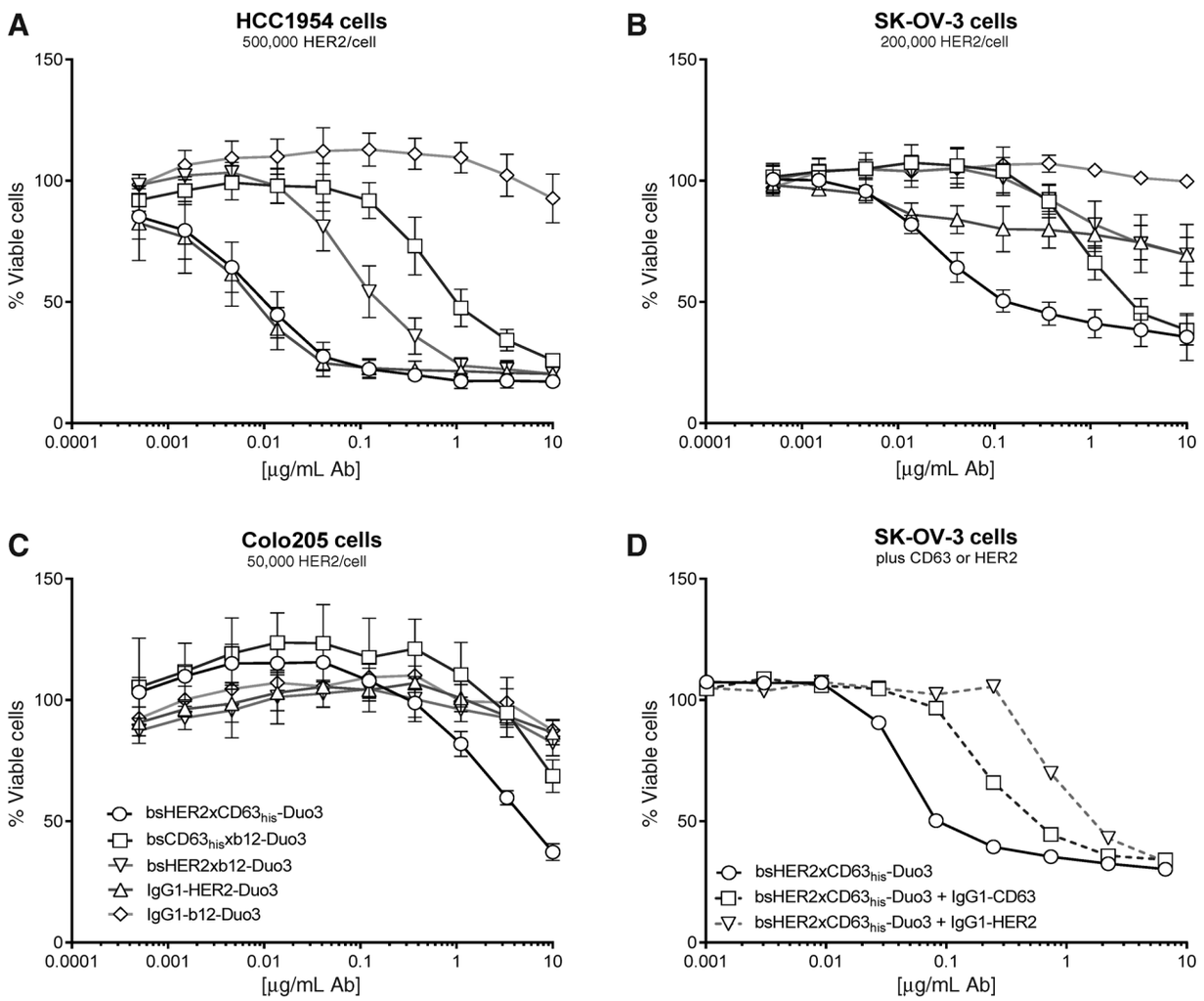

Figure 5.

Cytotoxicity of bsHER2xCD63$_{his}$-Duo3, bsHER2xb12-Duo3, bsCD63$_{his}$xb12-Duo3, IgG1 HER2-Duo3, and IgG1 b12-Duo3 *in vitro*. HCC1954 (**A**), SK-OV-3 (**B),** and Colo205 (**C**) cells were seeded in 96-well tissue culture plates together with serially diluted ADCs. SK-OV-3 (**D**) cells were also incubated with serially diluted ADCs plus 10 μg/mL unconjugated IgG1-HER2 or IgG1-CD63. After 3 days of incubation at 37°C viability was assessed using CellTiter-GLO and depicted as a percentage relative to untreated cells. **A–C,** data, mean ± standard deviation of at least 2 different experiments.

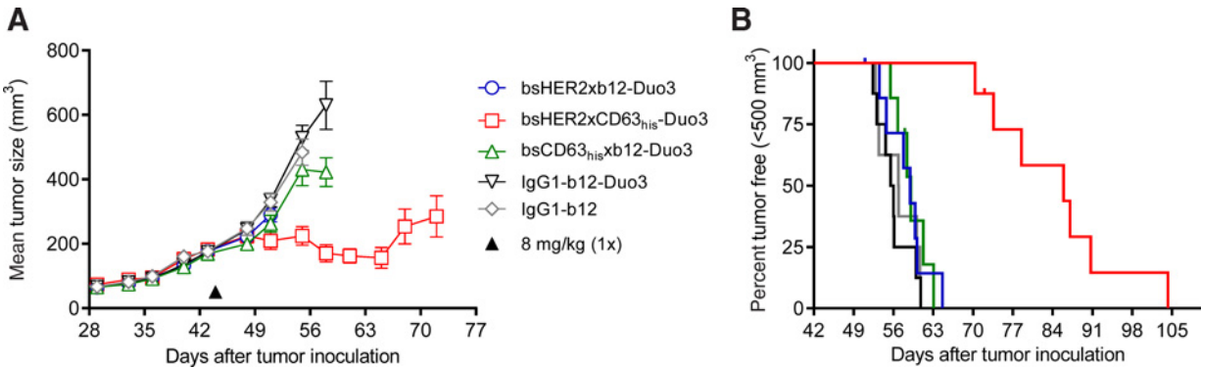

Figure 6.

Efficacy of bsHER2xCD63$_{his}$-Duo3, bsHER2xb12-Duo3, bsCD63$_{his}$xb12-Duo3, IgG1 b12-Duo3, and IgG1-b12 in a SK-OV-3 xenograft model. Mice were inoculated subcutaneously with 5 × 10^6 SK-OV-3 cells. When average tumor volume reached >200 mm^3, mice were divided in groups of 7 mice with equal tumor size distribution and injected intraperitoneally at indicated time points with 8 mg/kg ADC. Tumors were measured twice a week by using calipers, and the mean tumor volume ± SEM (mm^3) was plotted against time (**A**), as well as time to progression indicated by the percentage of mice with tumors <500 mm^3(**B**).

tumor growth, while the monovalent bsHER2xb12-ADC or bsCD63hisxb12-duo3 had no effect on tumor growth. This provides a strong proof-of-concept and demonstrates that a low-affinity CD63-specific Fab arm can be used to induce lysosomal delivery and toxin release of a poorly internalizing ADC in tumors *in vivo*.

Discussion

In the present study, we tested the possibility of enhancing lysosomal delivery of ADCs by targeting a tumor-specific antigen in combination with an antigen that facilitates trafficking to the lysosomes. To this end, a bsADC was generated that combines tumor-specific targeting through HER2, with enhanced lysosomal delivery through CD63. The binding affinity of the CD63 arm was modified in order to limit monovalent target binding and to direct the targeting characteristics of the bsAb to tumor cells that coexpress HER2 and CD63. The resulting bsHER2xCD63$_{his}$ demonstrated binding and lysosomal accumulation into HER2-positive tumor cells, but not CD63-positive granulocytes or thrombocytes. By conjugating bsHER2xCD63$_{his}$ with Duostatin-3, we were able to generate an ADC that induced *in vitro* and *in vivo* cytotoxicity of HER2-positive tumor cells. While treatment with monovalent CD63 and HER2 ADCs had no effect on growth of SK-OV-3 tumors *in vivo*, bsHER2xCD63$_{his}$-ADC showed clear inhibition of tumor growth. This demonstrates that a bispecific Fab arm recognizing an antigen involved in intracellular trafficking can be used in combination with a tumor-specific Fab arm, to facilitate intracellular delivery of ADCs.

The use of bispecific antibodies to improve efficacy of ADCs has been investigated by others previously. However, by recognizing two separate tumor-specific targets, these bsADCs were designed to target tumors with heterogeneous target expression. Thus, the ADCs would be able to recognize and kill tumors that express either one of the tumor targets, or both, broadening antitumor activity and reducing escape from therapy. A bispecific fusion protein targeting epithelial cell adhesion molecule (EpCAM) and CD133 was investigated in preclinical studies to deliver a bacterial toxin to EpCAM-positive tumor cells as well as cancer stem cells expressing CD133 (28). Similarly, a fusion protein targeting the EGF receptor and the urokinase receptor (uPAR) was used to target tumor cells through EGFR and tumor stroma through uPAR (29). DT2219, a bispecific recombinant immunotoxin targeting CD19 and CD22 positive B-cell tumors, demonstrated broader reactivity against B-cell malignancies as compared to individual immunotoxins targeting CD19 or CD22 alone (30, 31).

Our bsHER2xCD63$_{his}$-ADC has a different mechanism of action and can induce efficient cytotoxicity only when both antigens are expressed on the same cell. However, this approach can be applied to tumor antigens with poor or suboptimal internalization, thereby strongly expanding the number of tumor antigens that could be targeted by an ADC. For HER2, an antigen that only shows antibody induced downmodulation at high expression levels, bsHER2xCD63$_{his}$ was able to induce downmodulation of HER2 even on low HER2-expressing cell lines. This suggests that this approach may also be applicable to cell lines expressing low copy numbers of the targeted tumor antigen. However, exposure of Colo205 cells to bsHER2xCD63-ADC did not result in substantial cytotoxicity despite downmodulation of HER2 on these cells. This may in part be due to the low drug-to-antibody ratio (DAR) of our ADCs. Tubulin inhibitor–conjugated antibodies usually contain on average 3 to 4 drug molecules per antibody (32), while our ADCs had a DAR of one. Increasing the DAR of bsHER2xCD63-ADC may therefore result in further improving the cytotoxicity so that low HER2-expressing tumor cells can also be killed. However, as more potent ADCs might also affect normal cells expressing low levels of HER2, the decreased therapeutic window of such constructs should be carefully considered.

Another explanation for the lack of efficacy against low HER2-expressing tumors may be related to the mechanism of action of bsHER2xCD63$_{his}$-ADC. The affinity of the CD63-specific Fab arm was reduced to prevent uptake of bsHER2xCD63$_{his}$-ADC by healthy tissues that express CD63 (10, 19). On tumor cell lines that also expressed high numbers of HER2 molecules, CD63 binding was restored. We hypothesize that on these cells, bsHER2xCD63$_{his}$-ADC first bound to HER2, resulting in high density of bsHER2xCD63$_{his}$-ADC on the plasma membrane (Supplementary Fig. S3). This enabled bsHER2xCD63$_{his}$-ADC to bind to CD63 once it shuttles to the plasma membrane. On cell

lines with low HER2 expression, the likelihood that HER2 and CD63 binding occurs simultaneously is probably lower, because the proximity between both receptors is decreased. As a consequence, bsHER2xCD63$_{his}$-ADC can no longer bind to both HER2 and CD63. On the other hand, Fig. 3C shows that bsHER2xCD63$_{his}$ is also able to reduce HER2 levels on low HER2-expressing Colo205 cells.

There are no reports describing complex formation between HER2 and CD63. While CD63 expression at the plasma membrane has been described to concentrate to tetraspanin-enriched microdomains (33), HER2 has been described to localize to lipid rafts (34). A proteomics approach used to identify proteins in lipid rafts did not reveal any tetraspanins amongst the 241 identified proteins (35). Thus, at low copy number both receptors may very well be expressed in different microdomains at the cell surface. Selection of tumor-specific antigens that are known to interact with CD63 may improve bivalent binding of bsADC at low copy numbers. For example, CD63 has been described to interact with other tetraspanins (CD81, CD82, CD9, and CD151), integrins, MHCII, CXCR4, TM4SF5, syntenin-1, TIMP-1, H, K-ATPase, and MT1-MMP (10). Furthermore, antigens that are highly overexpressed, but lack lysosomal transport, may also represent attractive candidates. Glycosylphosphatidylinositol (GPI) anchored proteins (3, 36), adhesion molecules (6) and integrins (7) often recycle back to the plasma membrane after endocytosis, with only a minor fraction being targeted for lysosomal degradation. Using HER2 as a model antigen we have demonstrated that such antigens can be redirected for lysosomal degradation by a bsAb that also targets an antigen that is involved in intracellular trafficking CD63. Hence, these antigens may represent attractive targets for the development of a bsADC that combines tumor-specific targeting with enhanced lysosomal delivery through CD63.

Disclosure of Potential Conflicts of Interest

B.E.C.G. de Goeij, T. Vink, H. ten Napel, and P.W.H.I. Parren have ownership interest (including patents) in Genmab. No potential conflicts of interest were disclosed by the other authors.

Authors' Contributions

Conception and design: B.E.C.G. de Goeij, T. Vink, D. Satijn, P.W.H.I. Parren
Development of methodology: B.E.C.G. de Goeij, T. Vink, H. ten Napel, D. Miao, P.W.H.I. Parren
Acquisition of data (provided animals, acquired and managed patients, provided facilities, etc.): B.E.C.G. de Goeij, H. ten Napel, R. Wubbolts
Analysis and interpretation of data (e.g., statistical analysis, biostatistics, computational analysis): B.E.C.G. de Goeij, H. ten Napel, D. Satijn, P.W.H.I. Parren
Writing, review, and/or revision of the manuscript: B.E.C.G. de Goeij, T. Vink, D. Satijn, P.W.H.I. Parren
Administrative, technical, or material support (i.e., reporting or organizing data, constructing databases): B.E.C.G. de Goeij, R. Wubbolts
Study supervision: P.W.H.I. Parren

Acknowledgments

We would like to thank Ester van't Veld for technical support.

The costs of publication of this article were defrayed in part by the payment of page charges. This article must therefore be hereby marked *advertisement* in accordance with 18 U.S.C. Section 1734 solely to indicate this fact.

Received June 7, 2016; revised August 2, 2016; accepted August 2, 2016; published OnlineFirst August 24, 2016.

References

1. Burris HA. Developments in the use of antibody-drug conjugates. Am Soc Clin Oncol Educ Book 2013. doi: 10.1200/EdBook_AM.2013.33.e99.
2. Perez HL, Cardarelli PM, Deshpande S, Gangwar S, Schroeder GM, Vite GD, et al. Antibody-drug conjugates: current status and future directions. Drug Discov Today 2014;19:869–81.
3. Dautry-Varsat A, Ciechanover A, Lodish HF. pH and the recycling of transferrin during receptor-mediated endocytosis. Proc Natl Acad Sci U S A 1983;80:2258–62.
4. Harari D, Yarden Y. Molecular mechanisms underlying ErbB2/HER2 action in breast cancer. Oncogene 2000;19:6102–14.
5. Baulida J, Kraus MH, Alimandi M, Di Fiore PP, Carpenter G. All ErbB receptors other than the epidermal growth factor receptor are endocytosis impaired. J Biol Chem 1996;271:5251–7.
6. Kamiguchi H, Lemmon V. Recycling of the cell adhesion molecule L1 in axonal growth cones. J Neurosci 2000;20:3676–86.
7. Pellinen T, Ivaska J. Integrin traffic. J Cell Sci 2006;119:3723–31.
8. de Goeij BE, Satijn D, Freitag CM, Wubbolts R, Bleeker WK, Khasanov A, et al. High turnover of tissue factor enables efficient intracellular delivery of antibody-drug conjugates. Mol Cancer Ther 2015;14:1130–40.
9. Labrijn AF, Meesters JI, de Goeij BE, van den Bremer ET, Neijssen J, van Kampen MD, et al. Efficient generation of stable bispecific IgG1 by controlled Fab-arm exchange. Proc Natl Acad Sci U S A 2013;110:5145–50.
10. Pols MS, Klumperman J. Trafficking and function of the tetraspanin CD63. Exp Cell Res 2009;315:1584–92.
11. Duffield A, Kamsteeg EJ, Brown AN, Pagel P, Caplan MJ. The tetraspanin CD63 enhances the internalization of the H,K-ATPase beta-subunit. Proc Natl Acad Sci U S A 2003;100:15560–5.
12. Takino T, Miyamori H, Kawaguchi N, Uekita T, Seiki M, Sato H. Tetraspanin CD63 promotes targeting and lysosomal proteolysis of membrane-type 1 matrix metalloproteinase. Biochem Biophys Res Commun 2003;304:160–6.
13. Tugues S, Honjo S, Konig C, Padhan N, Kroon J, Gualandi L, et al. Tetraspanin CD63 promotes vascular endothelial growth factor receptor 2-beta1 integrin complex formation, thereby regulating activation and downstream signaling in endothelial cells in vitro and in vivo. J Biol Chem 2013;288:19060–71.
14. Janvier K, Bonifacino JS. Role of the endocytic machinery in the sorting of lysosome-associated membrane proteins. Mol Biol Cell 2005;16:4231–42.
15. Jelovac D, Emens LA. HER2-directed therapy for metastatic breast cancer. Oncology (Williston Park) 2013;27:166–75.
16. de Goeij BE, Peipp M, de Haij S, van den Brink EN, Kellner C, Riedl T, et al. HER2 monoclonal antibodies that do not interfere with receptor heterodimerization-mediated signaling induce effective internalization and represent valuable components for rational antibody-drug conjugate design. MAbs 2014;6:392–402.
17. Albanell J, Codony J, Rovira A, Mellado B, Gascon P. Mechanism of action of anti-HER2 monoclonal antibodies: scientific update on trastuzumab and 2C4. Adv Exp Med Biol 2003;532:253–68.
18. Li JY, Perry SR, Muniz-Medina V, Wang X, Wetzel LK, Rebelatto MC, et al. A biparatopic HER2-targeting antibody-drug conjugate induces tumor regression in primary models refractory to or ineligible for HER2-targeted therapy. Cancer Cell 2016;29:117–29.
19. Metzelaar MJ, Schuurman HJ, Heijnen HF, Sixma JJ, Nieuwenhuis HK. Biochemical and immunohistochemical characteristics of CD62 and CD63 monoclonal antibodies. Expression of GMP-140 and LIMP-CD63 (CD63 antigen) in human lymphoid tissues. Virchows Arch B Cell Pathol Incl Mol Pathol 1991;61:269–77.
20. Vink T, Oudshoorn-Dickmann M, Roza M, Reitsma JJ, de Jong RN. A simple, robust and highly efficient transient expression system for producing antibodies. Methods 2014;65:5–10.
21. Labrijn AF, Meesters JI, Priem P, de Jong RN, van den Bremer ET, van Kampen MD, et al. Controlled Fab-arm exchange for the generation of stable bispecific IgG1. Nat Protoc 2014;9:2450–63.

22. Parren PW, Ditzel HJ, Gulizia RJ, Binley JM, Barbas CF3rd, Burton DR, et al. Protection against HIV-1 infection in hu-PBL-SCID mice by passive immunization with a neutralizing human monoclonal antibody against the gp120 CD4-binding site. AIDS 1995;9:F1–6.
23. Igawa T, Ishii S, Tachibana T, Maeda A, Higuchi Y, Shimaoka S, et al. Antibody recycling by engineered pH-dependent antigen binding improves the duration of antigen neutralization. Nat Biotechnol 2010;28: 1203–7.
24. Chaparro-Riggers J, Liang H, DeVay RM, Bai L, Sutton JE, Chen W, et al. Increasing serum half-life and extending cholesterol lowering in vivo by engineering antibody with pH-sensitive binding to PCSK9. J Biol Chem 2012;287:11090–7.
25. Margadant C, Monsuur HN, Norman JC, Sonnenberg A. Mechanisms of integrin activation and trafficking. Curr Opin Cell Biol 2011;23:607–14.
26. Arjonen A, Alanko J, Veltel S, Ivaska J. Distinct recycling of active and inactive beta1 integrins. Traffic 2012;13:610–25.
27. Doronina SO, Toki BE, Torgov MY, Mendelsohn BA, Cerveny CG, Chace DF, et al. Development of potent monoclonal antibody auristatin conjugates for cancer therapy. Nat Biotechnol 2003;21:778–84.
28. Waldron NN, Barsky SH, Dougherty PR, Vallera DA. A bispecific EpCAM/CD133-targeted toxin is effective against carcinoma. Target Oncol 2014;9: 239–49.
29. Oh S, Tsai AK, Ohlfest JR, Panoskaltsis-Mortari A, Vallera DA. Evaluation of a bispecific biological drug designed to simultaneously target glioblastoma and its neovasculature in the brain. J Neurosurg 2011;114:1662–71.
30. Vallera DA, Oh S, Chen H, Shu Y, Frankel AE. Bioengineering a unique deimmunized bispecific targeted toxin that simultaneously recognizes human CD22 and CD19 receptors in a mouse model of B-cell metastases. Mol Cancer Ther 2010;9:1872–83.
31. Bachanova V, Frankel AE, Cao Q, Lewis D, Grzywacz B, Verneris MR, et al. Phase I study of a bispecific ligand-directed toxin targeting CD22 and CD19 (DT2219) for refractory B-cell malignancies. Clin Cancer Res 2015;21: 1267–72.
32. Lewis Phillips GD, Li G, Dugger DL, Crocker LM, Parsons KL, Mai E, et al. Targeting HER2-positive breast cancer with trastuzumab-DM1, an antibody–cytotoxic drug conjugate. Cancer Res 2008;68: 9280–90.
33. Nydegger S, Khurana S, Krementsov DN, Foti M, Thali M. Mapping of tetraspanin-enriched microdomains that can function as gateways for HIV-1. J Cell Biol 2006;173:795–807.
34. Nagy P, Vereb G, Sebestyen Z, Horvath G, Lockett SJ, Damjanovich S, et al. Lipid rafts and the local density of ErbB proteins influence the biological role of homo- and heteroassociations of ErbB2. J Cell Sci 2002;115:4251–62.
35. Foster LJ, De Hoog CL, Mann M. Unbiased quantitative proteomics of lipid rafts reveals high specificity for signaling factors. Proc Natl Acad Sci U S A 2003;100:5813–8.
36. Gamage DG, Hendrickson TL. GPI transamidase and GPI anchored proteins: oncogenes and biomarkers for cancer. Crit Rev Biochem Mol Biol 2013;48:446–64.